Extraordinary mechanical performance in charged carbyne

Yong-Zhe Guo(郭雍哲), Yong-Heng Wang(汪永珩), Kai Huang(黄凯), Hao Yin(尹颢)†, and En-Lai Gao(高恩来)‡

Citation: Chin. Phys. B, 2022, 31 (**12**): 128102. DOI: 10.1088/1674-1056/ac7bf8
Journal homepage: http://cpb.iphy.ac.cn; http://iopscience.iop.org/cpb

What follows is a list of articles you may be interested in

Stability and optoelectronic property of low-dimensional organic tin bromide perovskites

J H Lei(雷军辉), Q Tang(汤琼), J He(何军), and M Q Cai(蔡孟秋)
Chin. Phys. B, 2021, 30 (**3**): 038102. DOI: 10.1088/1674-1056/abc545

Dependence of mechanical properties on the site occupancy of ternary alloying elements in γ'-Ni_3Al: *Ab initio* description for shear and tensile deformation

Minru Wen(文敏儒), Xing Xie(谢兴), Huafeng Dong(董华锋), Fugen Wu(吴福根), Chong-Yu Wang(王崇愚)
Chin. Phys. B, 2020, 29 (**7**): 078103. DOI: 10.1088/1674-1056/ab8a38

Prediction of structured void-containing 1T-$PtTe_2$ monolayer with potential catalytic activity for hydrogen evolution reaction

Bao Lei(雷宝), Yu-Yang Zhang(张余洋), Shi-Xuan Du(杜世萱)
Chin. Phys. B, 2020, 29 (**5**): 058104. DOI: 10.1088/1674-1056/ab8203

Germanene nanomeshes:Cooperative effects of degenerate perturbation and uniaxial strain on tuning bandgap

Yan Su(苏燕), Xinyu Fan(范新宇)
Chin. Phys. B, 2017, 26 (**10**): 108101. DOI: 10.1088/1674-1056/26/10/108101

Fluctuations of electrical and mechanical properties of diamond induced by interstitial hydrogen

Zhuang Chun-Qiang (庄春强), Liu Lei
Chin. Phys. B, 2015, 24 (**1**): 018101. DOI: 10.1088/1674-1056/24/1/018101

SPECIAL TOPIC — The third carbon: Carbyne with one-dimensional sp-carbon

Extraordinary mechanical performance in charged carbyne

Yong-Zhe Guo(郭雍哲), Yong-Heng Wang(汪永珩), Kai Huang(黄凯), Hao Yin(尹颢)[†], and En-Lai Gao(高恩来)[‡]

Department of Engineering Mechanics, School of Civil Engineering, Wuhan University, Wuhan 430072, *China*

(Received 6 April 2022; revised manuscript received 22 June 2022; accepted manuscript online 27 June 2022)

Carbyne, the linear chain of carbon, promises the strongest and toughest material but possesses a Peierls instability (alternating single-bonds and triple-bonds) that reduces its strength and toughness. Herein, we computationally found that the gravimetric strength, strain-to-failure, and gravimetric toughness can be improved from 74 GPa·g^{-1}·cm^3, 18%, and 9.4 kJ·g^{-1} for pristine carbyne to the highest values of 106 GPa·g^{-1}·cm^3, 26%, and 19.0 kJ·g^{-1} for carbyne upon hole injection of +0.07 e/atom, indicating the charged carbyne with record-breaking mechanical performance. Based on the analyses of the atomic and electronic structures, the underlying mechanism behind the record-breaking mechanical performance was revealed as the suppressed and even eliminated bond alternation of carbyne upon charge injection.

Keywords: charged carbyne, first-principles calculations, strength and toughness, bond alternation

PACS: 81.05.U–, 36.20.Hb, 33.15.Fm **DOI:** 10.1088/1674-1056/ac7bf8

1. Introduction

Carbon allotropes have been widely explored and used in various fields of science and technology for the last few decades. In addition to the well-known two-dimensional (2D) graphene[1,2] and three-dimensional (3D) diamond,[3,4] one-dimensional (1D) carbon chains, carbyne, has also attracted increasing attention,[5,6] since carbyne with an extreme structure has been predicted to have extreme properties.[7–11] However, carbyne has a higher energy than graphite carbon because of sp^1 hybridization, making the fabrication of such material challenging.[12–14] Fortunately, carbyne formed at high temperatures and pressures was indicated in interstellar dust and meteorites,[15–18] and experimentalists have developed several methods for fabricating carbyne chains or segments, such as bulk production of long carbyne chains inside double-walled carbon nanotubes,[19] deriving carbyne segments from graphene,[20] synthesis of confined carbyne,[21] and synthesis of carbyne on metal surface or within evaporating liquid carbon.[22,23]

Mechanical strength and toughness are of fundamental importance for applications of carbyne, such as assembling strongest fibrous materials[24] and constructing angstrom-scale devices.[25,26] For example, Gao *et al.*[24] proposed a carbon assembly including a large carbyne bundle that is confined within a carbon nanotube sheath, in which the nanotube sheath protects the carbyne bundles against reaction, while the carbyne chains act as stiffening structures. The highest Young's modulus and gravimetric Young's modulus of this assembly were determined as 1505 GPa and 977 GPa·g^{-1}·cm^3, much higher than any known fibrous materials. This ultra-high performance of the assembly mainly results from the extreme mechanical properties of carbyne chains that have been well identified from both calculations and experiments. Liu *et al.*[7] first-principles calculated that the breaking force of carbyne chains is as high as 11.7 nN, corresponding to a tensile strength of 2500 GPa when a diameter of 0.77 Å was used and gravimetric strength of 75 GPa·g^{-1}·cm^3. Mikhailovskij *et al.*[8] *in-situ* measured the breaking force of carbyne chains as 11.2 nN, corresponding to a tensile strength of 245 GPa when a diameter of 2.4 Å was adopted and gravimetric strength of 72 GPa·g^{-1}·cm^3. These results indicate the breaking force and gravimetric strength of carbyne chains obtained from high-field calculations and experiments are generally consistent, while the reported tensile strength of carbyne chains are controversial mainly because of the variations in determining the cross-sectional area.[27] To avoid such controversy and make comparison with other materials, we use gravimetric measures, *e.g.*, gravimetric strength, to quantify the mechanical performance in this work.

The predicted gravimetric strength (74 GPa·g^{-1}·cm^3) and gravimetric toughness (9.4 kJ·g^{-1}) of carbyne chains are much greater than any known carbon allotropes, including diamond (24 GPa·g^{-1}·cm^3 and 2.0 kJ·g^{-1}) and graphene (51 GPa·g^{-1}·cm^3 and 8.8 kJ·g^{-1}).[28] The underlying mechanism is that chemical bonds of carbyne chains are stiff and aligned in the same direction, which endows carbyne with the mechanical supremacy over other materials. However, the stable form of carbyne (–C≡C–) contains alternating weak single-bonds and strong triple-bonds,[7,27,29–32] and the bond alternation increases with tensile strains, known as a Peierls

[†]Corresponding author. E-mail: yinhao@whu.edu.cn
[‡]Corresponding author. E-mail: enlaigao@whu.edu.cn

instability, which ultimately causes the premature fracture of carbyne from the breaking of long and weak bonds.[7]

Although the bond alternation greatly reduces the mechanical performance of carbyne, it still holds the records for the strength and toughness of materials. If the bond alternation can be eliminated for carbyne chains, these records of mechanical performance can be further improved. Considering that the bond alternation of carbyne originates from the electron density distribution between atoms, we wonder whether the electron density distribution can be engineered to suppress and even eliminate the bond alternation. Fortunately, Casari *et al.*[33] experimentally indicated that the bond length alternation of charged carbon-atom wires decreased. More recently, it was found that graphene,[34] graphene oxide,[35] phosphorene,[24] and Ti_2C MXene[36] upon charge injection exhibit extraordinary electromechanical actuation performance, and the mechanical properties of such materials can be modulated by charge injection.[36,37] Several charge injection methods have been reported, such as immersing carbon nanotube in an electrolyte and apply potential,[38] charge transfer between carbon wires and metal nanoparticles,[39] and nitrogen doped carbyne.[40] These results provide an indication for obtaining record-breaking mechanical performance by charge-engineering carbyne chains.

In this work, we investigated the mechanical performance of charged carbyne by using first-principles calculations. It was found that the gravimetric strength, strain-to-failure, gravimetric toughness, and breaking force can be improved from 74 GPa·g^{-1}·cm^3, 18%, 9.4 kJ·g^{-1}, and 11.5 nN for pristine carbyne to the highest values of 106 GPa·g^{-1}·cm^3, 26%, 19.0 kJ·g^{-1}, and 16.5 nN for charged carbyne, making the charged carbyne the strongest and the toughest material. The mechanism analyses of bonding pattern and electronic structures show that the bonding alternation of carbyne under tension is suppressed and even eliminated by charge-engineering, which accounts for such record-breaking mechanical performance of charged carbyne.

2. Computational details

The calculations were conducted using density functional theory (DFT) implemented in the Vienna *ab-initio* simulation package (VASP).[41] Unless otherwise noted, the Perdew–Burke–Ernzerhof (PBE) parameterization[42] of the generalized gradient approximation (GGA)[43] was used for the exchange–correlation functional. For all the calculations in this work, energy cut-off of 520 eV was used, and *k*-point mesh with the density $>$ 80 Å (the product of each lattice constant and the corresponding number of *k*-points) was adopted for the Brillouin zone sampling.[44] All atomic positions and axial lattice parameters of the structures have been optimized until all forces were less than 0.01 eV/Å. Our calculations indicate that the calculated mechanical properties are almost independent on the axial sizes of computational cells (Fig. S1 in supporting information). Meanwhile, our calculations indicate that a vacuum layer over 40 Å has only slight effect on the mechanical properties (Fig. S2). To balance the computational accuracy and cost, a vacuum layer of 40 Å was adopted in this work. Considering a balance between accuracy and efficiency, energy cut-off of 400 eV, *k*-point mesh with the density of about 30 Å and vacuum layer of 20 Å was used in the *ab-initio* molecular dynamics (AIMD) simulations.

3. Results and discussion

3.1. Stabilities of charged carbyne

Density functional theory (DFT) calculations were used to investigate the stabilities of charged carbyne. By tracking the bond length alternation (BLA), internal dimerization for the pristine carbyne has been identified, since the polyyne structure (–C≡C–) is more stable than the cumulene structure (=C=C=).[30] The calculated energy barrier for the transition from the polyyne structure to the cumulene structure for pristine carbyne is 4 meV per atom (Fig. S3). Upon a certain amount of charge injection (-0.10 e/atom to $+0.10$ e/atom), carbyne still maintains linear bonding patterns, as illustrated in Fig. 1(a). Interestingly, the BLA decreases to zero as the charge injection increases to ± 0.07 e/atom, since the energy of the cumulene structure is lower than that of polyyne structure (Fig. S3). When the charge injection exceeds ± 0.07 e/atom, the carbyne chains show uniform bond lengths, indicating that these chains are free of Peierls instabilities.

Furthermore, we calculated the phonon dispersions for quantifying the dynamical stability of these structures (Fig. 1(b)). The absence of imaginary frequencies indicates the dynamical stability of the pristine carbyne and charged carbyne. Afterwards, the energy above convex hull was used to measure the stability of carbyne (the energy difference at zero pressure and zero temperature between the energy for charged carbyne and graphite). The calculated energy above convex hull values of carbyne upon charge injection of -0.07, 0.00, and $+0.07$ e/atom are 0.79, 1.03, and 1.52 eV/atom, respectively. This suggests that the likely ease of charged carbyne fabrication can be sequenced as electron injected carbyne $>$ pristine carbyne $>$ hole injected carbyne. Finally, we explored the thermodynamic stability by performing AIMD simulations (a supercell having 12 atoms) at 300 K for 10 ps. During the AIMD simulations, the pristine carbyne and charged carbyne maintain their structures with only slight lattice perturbation from thermal fluctuations (see Fig. S4 and movie S1 for details).

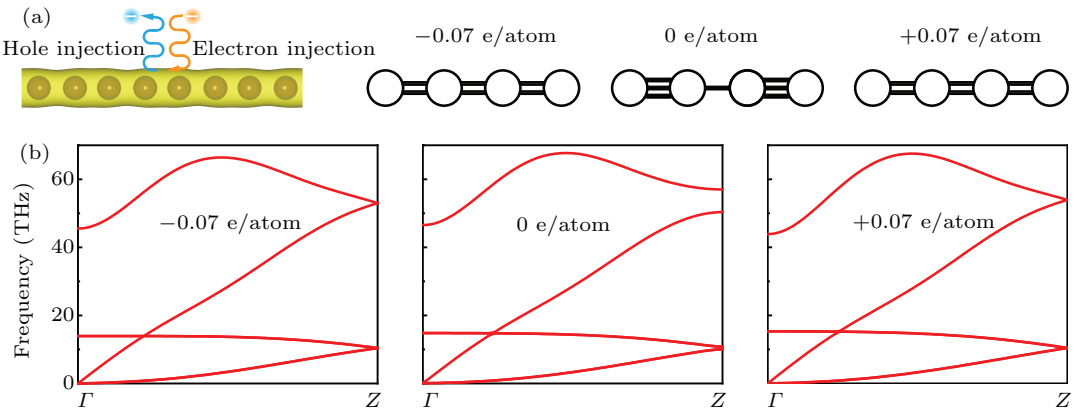

Fig. 1. Structures and stabilities of charged carbyne. (a) Illustration of charge injection into carbyne, and the bonding patterns for carbyne upon charge injection. (b) Phonon dispersions of pristine carbyne and charged carbyne upon electron injection of −0.07 e/atom and hole injection of +0.07 e/atom.

3.2. Mechanical properties of charged carbyne

To investigate the mechanical performance of carbyne upon charge injection, we calculated the force–strain and gravimetric stress–strain curves by using the DFT method (Fig. 2). Both calculations at local density approximation (LDA) and generalized gradient approximation (GGA) levels were performed for comparison. Calculations using these two approximations are in good agreement (Fig. S5). Our calculated gravimetric strength (74 GPa·g^{-1}·cm^3), breaking force (11.5 nN), and strain-to-failure (18%) for the pristine carbyne agree with those (75 GPa·g^{-1}·cm^3, 11.7 nN, and 18%) calculated by Yakobson's team.[7] The gravimetric strength, gravimetric toughness and gravimetric modulus for pristine carbyne and charged carbyne were summarized in Table S1.

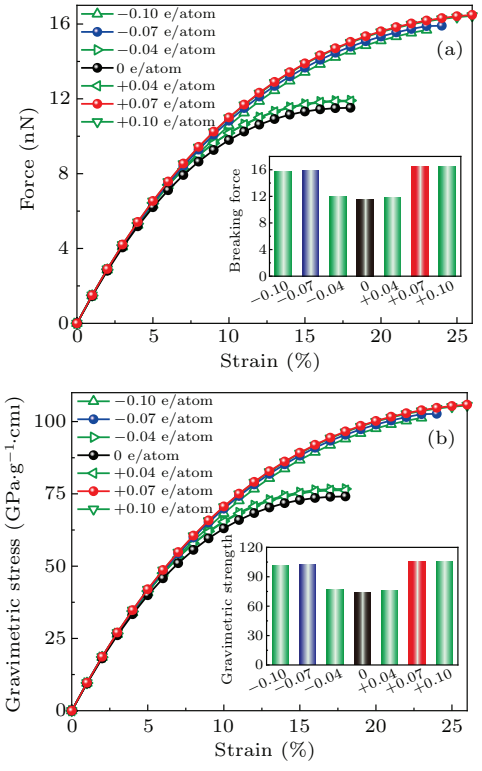

Fig. 2. Mechanical performance of pristine carbyne and charged carbyne. (a) Force *versus* strain and (b) gravimetric stress *versus* strain curves for pristine carbyne and charged carbyne.

The gravimetric strength, strain-to-failure, gravimetric toughness, and breaking force of carbyne significantly increase with charge injection before ±0.07 e/atom. Upon hole injection of +0.07 e/atom, the gravimetric strength, strain-to-failure, gravimetric toughness, and breaking force of carbyne increase to their highest values of 106 GPa·g^1·cm^3, 26%, and 19.0 kJ·g^{-1}, and 16.5 nN. In a contrast, the maximum gravimetric modulus of carbyne upon charge injection is only 3% higher than that of pristine carbyne, suggesting a slight modulation of stiffness by charge-engineering. The highest gravimetric modulus (967 GPa·g^{-1}·cm^3), gravimetric strength (106 GPa·g^{-1}·cm^3), and gravimetric toughness (19.0 kJ·g^{-1}) of charged carbyne is higher than those of pristine carbyne (939 GPa·g^{-1}·cm^3, 74 GPa·g^{-1}·cm^3, and 9.4 kJ·g^{-1}), graphene (453 GPa·g^{-1}·cm^3, 51 GPa·g^{-1}·cm^3, and 8.8 kJ·g^{-1}), and diamond (327 GPa·g^{-1}· cm^3, 24 GPa·g^{-1}·cm^3, and 2.0 kJ·g^{-1})[24] (Fig. 3). To our knowledge, the gravimetric modulus, gravimetric strength, and gravimetric toughness are higher than any reported materials in literature, making the optimally charged carbyne the stiffest, the strongest, and the toughest predicted material (Fig. 3).

The above-reported mechanical properties are investigated at the temperature of 0 K. Furthermore, we investigated the finite temperature effect on the mechanical properties of charged carbyne. At a finite temperature, the average failure rate for a single bond follows the Arrhenius form[45,46]

$$R(\sigma) = \nu(f)\,\mathrm{e}^{-\Delta E(\sigma)/k_{\mathrm{B}}T}, \tag{1}$$

where $\nu(f)$ is approximately 10^{13} Hz (the "attempt rate" to cross over the energy barrier), $\Delta E(\sigma)$ is the energy barrier to break a single bond, k_{B} and T are the Boltzmann constant and temperature, respectively. For atomic chains, the increasing failure rates of every single bond due to the increase of temperature would lead to the decrease in strength. From Eq. (1) and the calculated $\Delta E(\sigma)$ for charged carbyne, we predicted the relative strength (the averaged strength at a finite temperature divided by the averaged strength at the temperature of 0 K) as a function of temperature (Fig. S6).

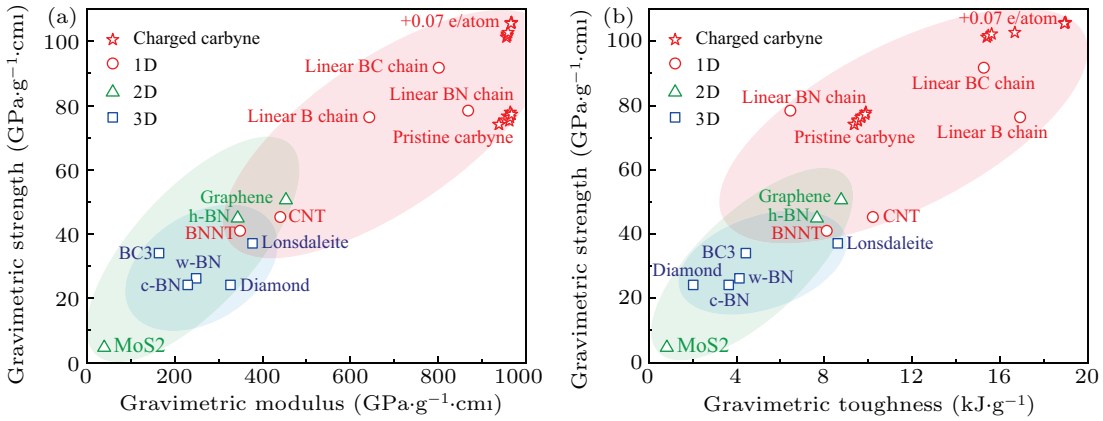

Fig. 3. Calculated modulus, strength, and toughness of typical high-mechanical-performance materials. (a) Gravimetric strength *versus* gravimetric modulus and (b) gravimetric strength *versus* gravimetric toughness of charged carbyne compared with other typical high-modulus, high-strength, and high-toughness materials.

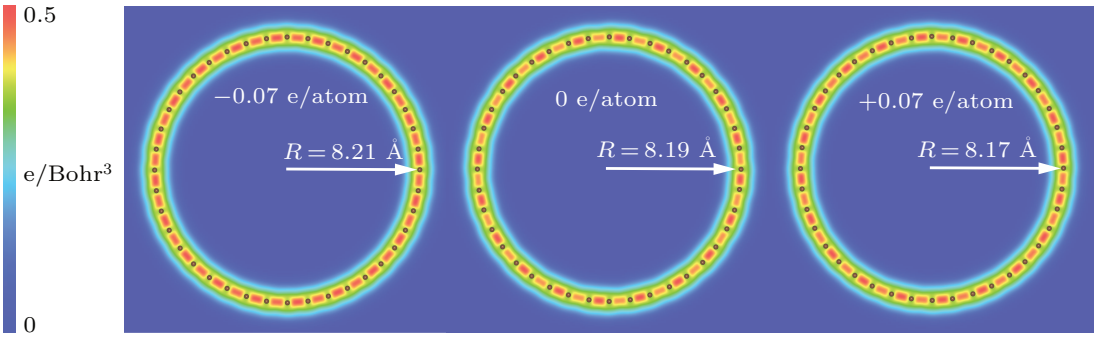

Fig. 4. Bending configurations of charged carbyne from DFT calculations.

Since the bending stiffness is useful for understanding the configurations of linear atomic chains in thermal fluctuations,[47–50] we calculate the bending stiffness of pristine charged carbyne for comparison with pristine carbyne. The bending stiffness (k_b) was obtained from the energy (E_b) for bending a long chain into a circle with radius R: $k_b = E_b R/\pi$.[51] Our calculated bending stiffness of pristine carbyne (3.7 eV·Å) agree with that (3.6 eV·Å) calculated by Yakobson's team.[7] The calculated bending stiffness for carbyne upon charge injection of −0.07 e/atom and +0.07 e/atom were 2.8 eV·Å and 1.6 eV·Å, respectively, indicating the increased bending flexibility compared with pristine carbyne. Additionally, it was found that the bond alternation in both linear and circular charged structures decreases with charge injection, and the radius of the circles slightly increases (decreases) with electron (hole) injection (Fig. 4).

3.3. Mechanism behind the superb mechanical performance of charged carbyne

To understand the mechanism behind the exceptional mechanical performance of charged carbyne, we did analyses at the atomic and electronic scales. First, the bonding structures of strain-free carbyne upon different charge injections were calculated. The bonds of charge-free carbyne were alternated into long bonds and short bonds. As the electron/hole injection increases, the averaged bond length slightly changes from 1.28 Å to 1.29 Å, while the bond length alternation (BLA) decreases to zero as the charge injection exceeds ±0.07 e/atom (Fig. 5(a)), indicating that the charge injection suppresses and even eliminates the BLA for strain-free carbyne. Considering that the BLA of carbyne predicted by DFT theory is generally underestimated, and Yang *et al.*[52] found that the accurate estimate of the BLA is 0.13 Å, we also did calculations using HSE06 functional for comparison. The BLA calculated using HSE06 functional is 0.1 Å, which is generally consistent with previous reported values.[53,54] Additionally, the calculations using HSE06 functional indicated that BLA keeps zero in the whole stretching process until strain-to-failure as the hole injection increases to +0.13 e/atom. In this case, the gravimetric strength, strain-to-failure, and breaking force of carbyne reaches their highest values of 115 GPa·g^{-1}·cm^3, 29%, and 18.0 nN. These results generally agree with the achieved record-breaking mechanical performance of charged carbyne calculated at GGA level. Hence, considering a balance between computational accuracy and efficiency, the following mechanism analyses were based on calculations at GGA level.

As charged carbyne was stretched, both the long bonds and short bonds were elongated. To quantify the bond deformation for carbyne, the local strains for the alternated long

bonds ($\varepsilon_{\rm L}$) and short bonds ($\varepsilon_{\rm S}$) were defined as

$$\varepsilon_{\rm L} = \frac{L_{\rm L} - L_{\rm L0}}{L_{\rm L0}}, \tag{2}$$

$$\varepsilon_{\rm S} = \frac{L_{\rm S} - L_{\rm S0}}{L_{\rm S0}}, \tag{3}$$

where $L_{\rm L0}$ ($L_{\rm L}$) and $L_{\rm S0}$ ($L_{\rm S}$) are the lengths of the long bonds and short bonds under zero strain (strain-to-failure), respectively. To quantify the contribution of long bonds and short bonds on the strain-to-failure of carbyne (ε), measures for the long bonds ($C_{\rm L}$) and short bonds ($C_{\rm S}$) were proposed as

$$C_{\rm S} = \frac{L_{\rm L} - L_{\rm L0}}{L_0 \varepsilon}, \tag{4}$$

$$C_{\rm S} = \frac{L_{\rm S} - L_{\rm S0}}{L_0 \varepsilon}, \tag{5}$$

where L_0 is the sum of lengths of the long and short bonds. Based on Eqs. (2)–(5), we calculated the local strains of long bonds and short bonds and measured their contribution on the strain-to-failure of carbyne (Fig. 5(b)). As the charge injected from -0.6 e/atom to $+0.06$ e/atom, the strains of long bonds and short bonds for carbyne are 32% and 3%–4%, respectively, and the contribution of long bonds to the strain-to-failure of carbyne exceeds 90%. These results indicate that the strain is largely localized in long bonds, accounting for the low strain-to-failure of carbyne upon these ranges of charge injections. As the charge injection exceeds ± 0.07 e/atom, the uniform strains of long bonds and short bonds contribute almost equally to the strain-to-failure of carbyne, which significantly improves the strain-to-failure of carbyne. Interestingly, although the initial bond length of carbyne upon hole injection of $+0.07$ e/atom is slightly shorter than that upon electron injection of -0.07 e/atom, the bond length at the strain-to-failure is reversed. These results explain the larger average bond strain (larger strain-to-failure) of carbyne upon hole injection of $+0.07$ e/atom than that upon electron injection of -0.07 e/atom. Considering that the gravimetric modulus almost keeps a constant value during charge injection (Fig. 2(b)), the increase of strain-to-failure explains the increase of gravimetric strength and gravimetric toughness.

Since bond patterns are intrinsically from the electron density distribution between atoms, we further calculated the electron density distribution (Fig. 6(a)). It can be observed that the electron density distribution between atoms for pristine carbyne alternates, indicating an alternated bonding pattern. As stretched to strain-to-failure, the electron density alternation increases. As the charge injection increases to ± 0.07 e/atom, the electron density distribution between atoms becomes uniform. Furthermore, we calculated the excess charge density distribution (Fig. 6(b)). For electron injection, excessive electrons largely accumulate in the long bonds, strengthening these weak bonds; for hole injection, excessive holes largely accumulate in the short bonds, weakening the strong bonds. As a result, the bond orders become uniform as charge injection increases (Fig. 6(a)). Therefore, the fundamental mechanism at the electron scale is the peak shaving and valley filling of electron density distribution (injecting excess holes into short, strong bonds and excess electrons into long, weak bonds upon hole injection and electron injection, respectively), which suppresses and even eliminates the bonding alternation of carbyne upon charge injection.

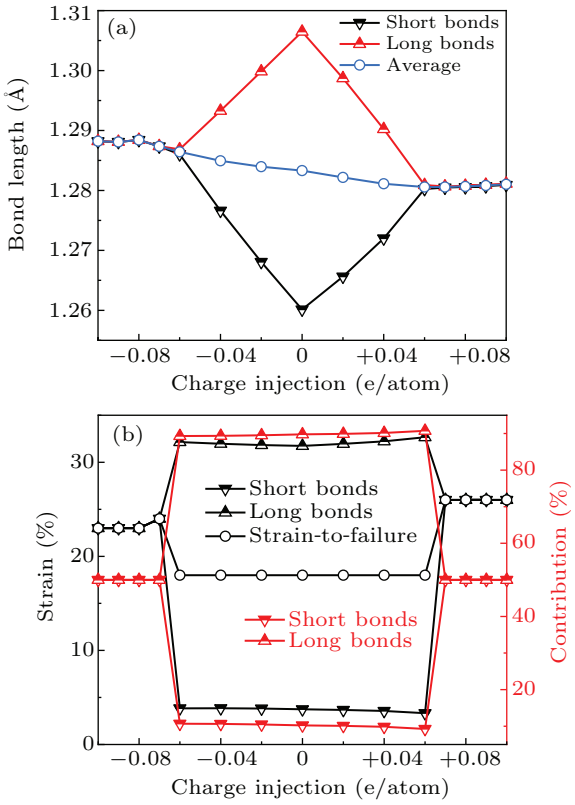

Fig. 5. Bonding pattern analysis of pristine carbyne and charged carbyne. (a) Bond lengths of strain-free charged carbyne. (b) Bond strain of long and short bonds and the contribution of these bonds to the strain-to-failure of carbyne.

Additionally, we calculated band structures for pristine and charged carbyne, which agrees Peierls-type semiconductor-to-metal transition (Fig. S7). The value of Fermi level is -5.31 eV for pristine carbyne. Upon charge injection, the values of Fermi level shift accordingly. As a result, the band gap of pristine carbyne is 0.42 eV, which is close to previous DFT calculations at PBE level,[56] while the band gap decreases from 0.42 eV to 0.00 eV as the charge injection increases to ± 0.07 e/atom, signaling a semiconductor-to-metal transitions. These results demonstrated a correlation between the semiconductor-to-metal transitions and a Peierls distortion.

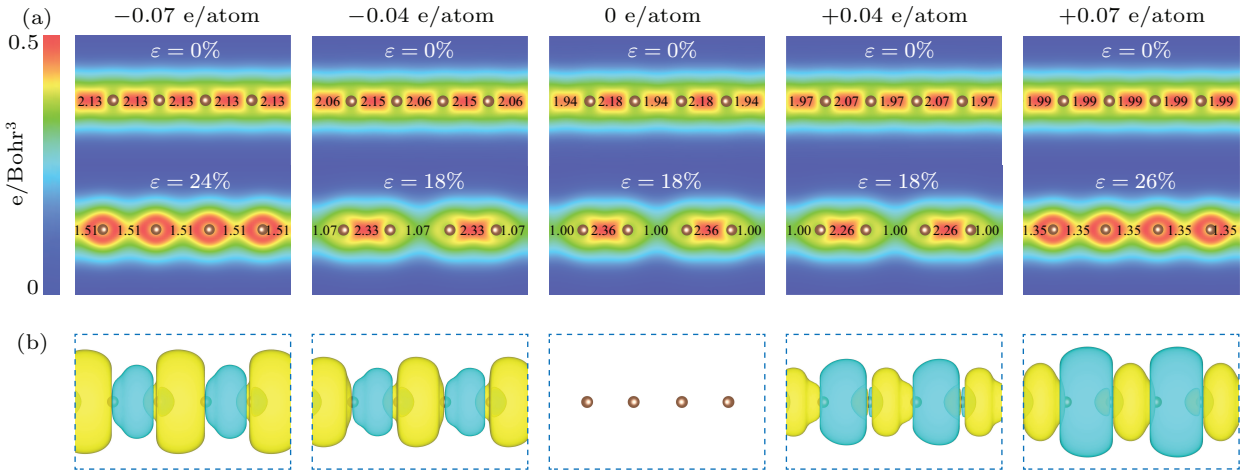

Fig. 6. Electronic structures of pristine carbyne and charged carbyne. (a) Electron density distribution of pristine carbyne and charged carbyne upon electron injection of −0.04, −0.07 e/atom and hole injection of +0.04, +0.07 e/atom under strain of 0% and strain-to-failure. The calculated bond orders[55] are labelled between atoms. (b) Excess charge density distribution for pristine carbyne and charged carbyne upon electron injection of −0.04, −0.07 e/atom and hole injection of +0.04, +0.07 e/atom, with the iso-surface values of 0.001 e/Bohr^3, under strain of 0% and strain-to-failure. Color coding of yellow and green represents excess electron and hole, respectively.

4. Conclusions

In summary, we computationally achieved record-breaking mechanical performance by demonstrating that charged carbyne chains have the known highest gravimetric strength and gravimetric toughness. The gravimetric strength, strain-to-failure, gravimetric toughness, and breaking force can be significantly improved from 74 GPa·g^{-1}·cm^3, 18%, 9.4 kJ·g^{-1}, and 11.5 nN for pristine carbyne to the highest values of 106 GPa·g^{-1}·cm^3, 26%, 19.0 kJ·g^{-1}, and 16.5 nN for carbyne upon hole injection of +0.07 e/atom. Some of which are near the theoretical bounds.[57] Further comparison with other high-mechanical-performance materials identified that carbyne upon the optimal charge injection has much higher gravimetric strength and gravimetric toughness than any know materials. The mechanism analyses revealed that the record-breaking mechanical properties of carbyne upon charge injection results from the peak shaving and valley filling of electron density distribution, which suppresses and even eliminates the bond alternation.

Acknowledgements

Project supported by the National Natural Science Foundation of China (Grant Nos. 12172261 and 11972263). The numerical calculations in this work have been performed on a supercomputing system in the Supercomputing Center of Wuhan University. Yongzhe Guo acknowledges the technical assistance from Chunbo Zhang and Xiangzheng Jia.

References

[1] Wan F, Wang X R, Liao L H, Zhang J Y, Chen M N, Zhou G H, Siu Z B, Jalil M B A and Li Y 2022 *Chin. Phys. B* **31** 077302
[2] Novoselov K S, Geim A K, Morozov S V, Jiang D, Zhang Y, Dubonos S V, Grigorieva I V and Firsov A A 2004 *Science* **306** 666
[3] Miao X Y, Ma H A, Zhang Z F, Chen L C, Zhou L J, Li M S and Jia X P 2021 *Chin. Phys. B* **30** 068102
[4] Telling R H, Pickard C J, Payne M C and Field J E 2000 *Phys. Rev. Lett.* **84** 5160
[5] Casari C S and Milani A 2018 *MRS Commun.* **8** 207
[6] Hirsch A 2010 *Nat. Mater.* **9** 868
[7] Liu M, Artyukhov V I, Lee H, Xu F and Yakobson B I 2013 *ACS Nano* **7** 10075
[8] Mikhailovskij I M, Sadanov E V, Kotrechko S, Ksenofontov V A and Mazilova T I 2013 *Phys. Rev. B* **87** 045410
[9] Li J P, Meng S H, Lu H T and Tohyama T 2018 *Chin. Phys. B* **27** 117101
[10] Gao E, Guo Y, Wang Z, Nielsen S O and Baughman R H 2022 *Matter* **5** 1192
[11] Zhan H and Gu Y 2018 *Chin. Phys. B* **27** 038103
[12] Prenzel D, Kirschbaum R W, Chalifoux W A, McDonald R, Ferguson M J, Drewello T and Tykwinski R R 2017 *Org. Chem. Front.* **4** 668
[13] Tykwinski R R, Chalifoux W, Eisler S, Lucotti A, Tommasini M, Fazzi D, Del Zoppo M and Zerbi G 2010 *Pure Appl. Chem.* **82** 891
[14] Baughman R H 2006 *Science* **312** 1009
[15] Webster A 1980 *Mon. Notices Royal Astron. Soc.* **192** 7
[16] Goresy A E and Donnay G 1968 *Science* **161** 363
[17] Hayatsu R, Scott R G, Studier M H, Lewis R S and Anders E 1980 *Science* **209** 1515
[18] Whittaker A G, Watts E J, Lewis R S and Anders E 1980 *Science* **209** 1512
[19] Shi L, Rohringer P, Suenaga K, Niimi Y, Kotakoski J, Meyer J C, Peterlik H, Wanko M, Cahangirov S, Rubio A, Lapin Z J, Novotny L, Ayala P and Pichler T 2016 *Nat. Mater.* **15** 634
[20] Jin C, Lan H, Peng L, Suenaga K and Iijima S 2009 *Phys. Rev. Lett.* **102** 205501
[21] Shi L, Senga R, Suenaga K, Chimborazo J, Ayala P and Pichler T 2021 *Carbon* **182** 348
[22] Cannella C B and Goldman N 2015 *J. Phys. Chem. C* **119** 21605
[23] Sun Q, Cai L, Wang S, Widmer R, Ju H, Zhu J, Li L, He Y, Ruffieux P, Fasel R and Xu W 2016 *J. Am. Chem. Soc.* **138** 1106
[24] Gao E, Li R and Baughman R H 2020 *ACS Nano* **14** 17071
[25] Kotrechko S, Timoshevskii A, Kolyvoshko E, Matviychuk Y and Stetsenko N 2017 *Nanoscale Res. Lett.* **12** 327
[26] Hou L, Hu H, Yang G and Ouyang G 2021 *Phys. Status Solidi - Rapid Res. Lett.* **15** 2000582
[27] Faria B, Bernardes C E S, Silvestre N and Canongia Lopes J N 2020 *Phys. Chem. Chem. Phys.* **22** 758
[28] Shao Q, Li R, Yue Z, Wang Y and Gao E 2021 *Chem. Mater.* **33** 1276
[29] Banhart F 2015 *Beilstein J. Nanotechnol.* **6** 559
[30] Kertesz M, Koller J and Aman A 1978 *J. Chem. Phys.* **68** 2779
[31] Liu X, Zhang G and Zhang Y W 2015 *J. Phys. Chem. C* **119** 24156
[32] Artyukhov V I, Liu M and Yakobson B I 2014 *Nano Lett.* **14** 4224
[33] Casari C S, Tommasini M, Tykwinski R R and Milani A 2016 *Nanoscale* **8** 4414
[34] Rogers G W and Liu J Z 2011 *J. Am. Chem. Soc.* **133** 10858
[35] Rogers G W and Liu J Z 2013 *Appl. Phys. Lett.* **102** 021903

[36] Wu B, Cai X, Shui L, Gao E and Liu Z 2020 *J. Phys. Chem. C* **125** 1060
[37] Wu B, Deng H X, Jia X, Shui L, Gao E and Liu Z 2020 *npj Comput. Mater.* **6** 27
[38] Baughman R H, Cui C, Zakhidov A A, Iqbal Z, Barisci J N, Spinks G M, Wallace G G, Mazzoldi A, De Rossi D, Rinzler A G, Jaschinski O, Roth S and Kertesz M 1999 *Science* **284** 1340
[39] Milani A, Lucotti A, Russo V, Tommasini M, Cataldo F, Li Bassi A and Casari C S 2011 *J. Phys. Chem. C* **115** 12836
[40] Liu Y, Wang W, Wang A, Jin Z, Zhao H and Yang Y 2017 *Electrochim. Acta* **232** 142
[41] Kresse G and Furthmuller J 1996 *Phys. Rev. B* **54** 11169
[42] Perdew J P, Burke K and Ernzerhof M 1996 *Phys. Rev. Lett.* **77** 3865
[43] Filippi C, Singh D J and Umrigar C J 1994 *Phys. Rev. B* **50** 14947
[44] Monkhorst H J and Pack J D 1976 *Phys. Rev. B* **13** 5188
[45] Puthur R and Sebastian K L 2002 *Phys. Rev. B* **66** 024304
[46] Charan H, Hansen A, Hentschel H G E and Procaccia I 2021 *Phys. Rev. Lett.* **126** 085501
[47] Maier W F, Lau G C and McEwen A B 1985 *J. Am. Chem. Soc.* **107** 4724
[48] Santiago C, Houk K N, DeCicco G J and Scott L T 1978 *J. Am. Chem. Soc.* **100** 692
[49] Zhang K, Zhang Y and Shi L 2020 *Chin. Chem. Lett.* **31** 1746
[50] Szafert S and Gladysz J A 2006 *Chem. Rev.* **106** 1
[51] Gao E and Xu Z 2015 *J. Appl. Mech.* **82** 121012
[52] Yang S and Kertesz M 2006 *J. Phys. Chem. A* **110** 9771
[53] Al-Backri A, Zolyomi V and Lambert C J 2014 *J. Chem. Phys.* **140** 104306
[54] Mostaani E, Monserrat B, Drummond N D and Lambert C J 2016 *Phys. Chem. Chem. Phys.* **18** 14810
[55] Manz T A 2017 *RSC Adv.* **7** 45552
[56] Cahangirov S, Topsakal M and Ciraci S 2010 *Phys. Rev. B* **82** 195444
[57] Gao E, Yuan X, Nielsen S O and Baughman R H 2022 *Phys. Rev. Appl.* **18** 014044

Supporting information

Extraordinary Mechanical Performance in Charged Carbyne

Yong-Zhe Guo (郭雍哲), Yong-Heng Wang (汪永珩), Kai Huang (黄凯), Hao Yin* (尹颢), and En-Lai Gao* (高恩来)

Department of Engineering Mechanics, School of Civil Engineering, Wuhan University, Wuhan, Hubei 430072, China.

*Corresponding authors. Emails: enlaigao@whu.edu.cn; yinhao@whu.edu.cn

The Appendix A contains:

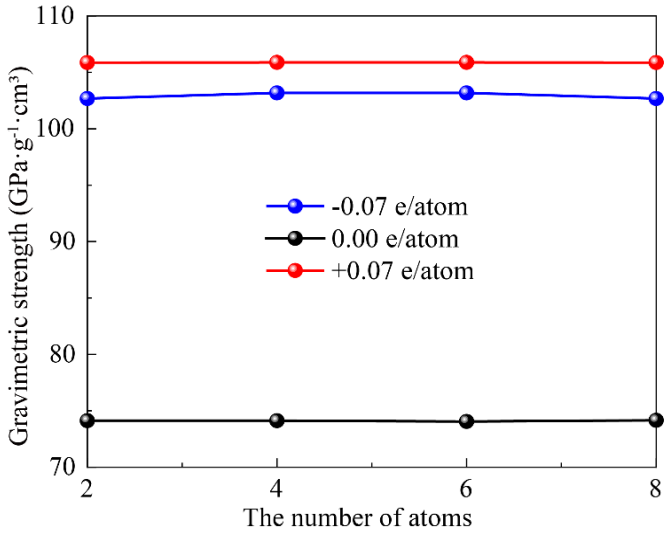

Fig. S1. Gravimetric strength of charge-engineered carbyne upon sizes of different computational models.

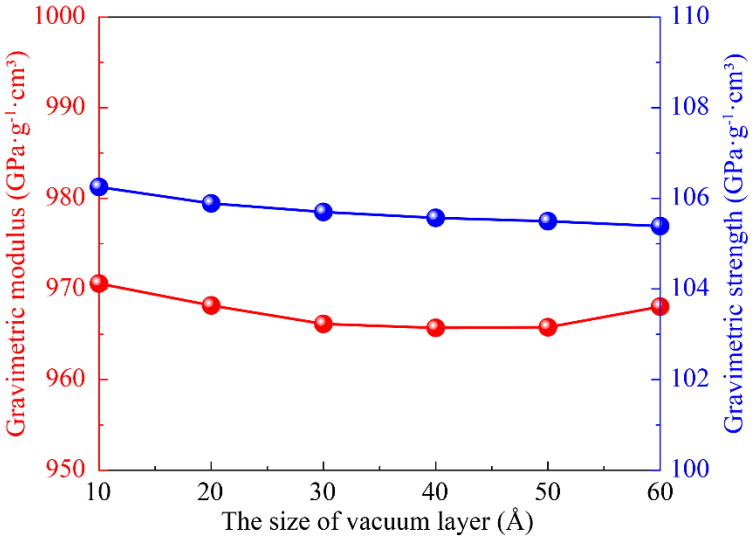

Fig. S2. Gravimetric modulus and gravimetric strength for charged carbyne using different sizes of vacuum layers.

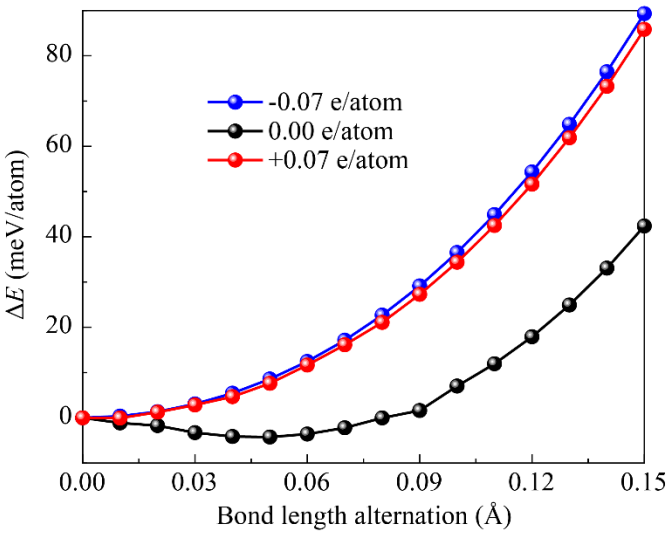

Fig. S3. Energy differences between alternating bonding and uniform bonding of charged and pristine carbyne.

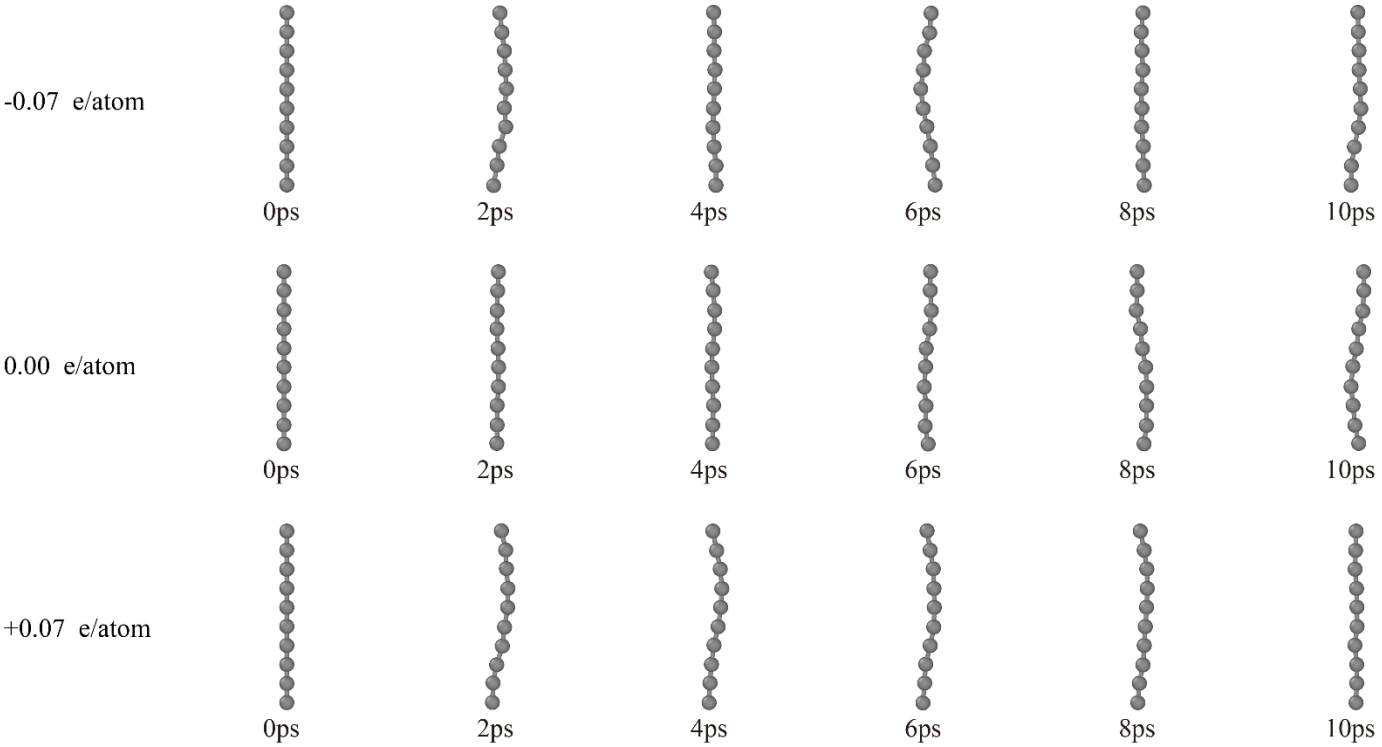

Fig. S4. Ab initio molecular dynamics simulation of carbyne upon charge injection of 0 and ±0.07 e/atom at 300 K for 10 ps.

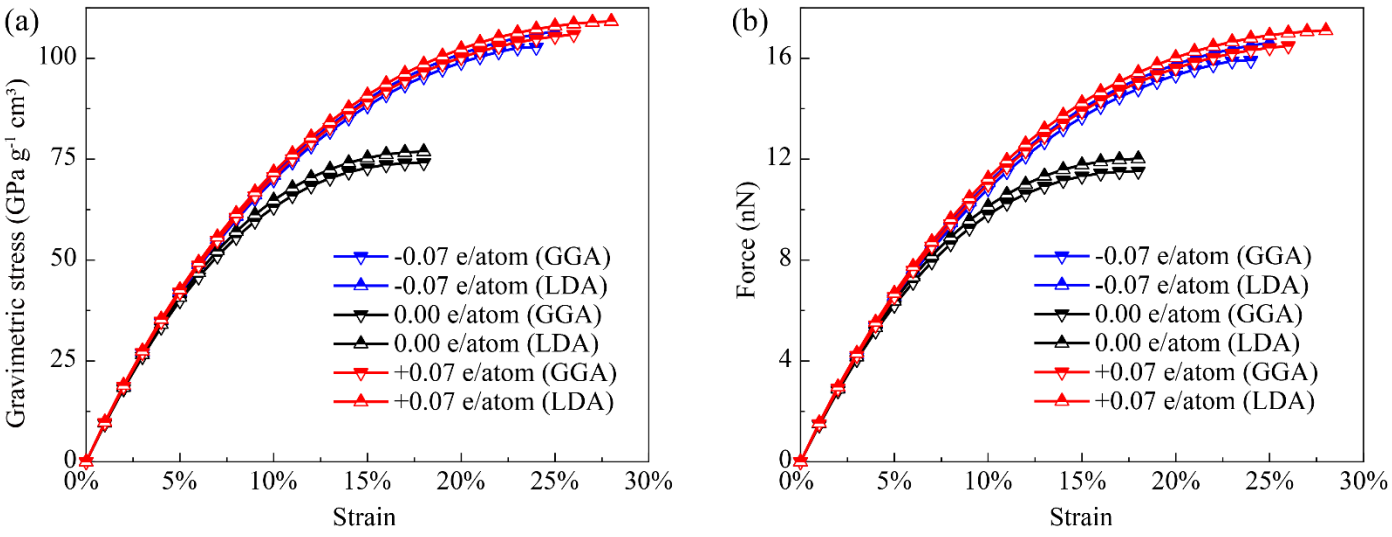

Fig. S5. (a) Gravimetric stress vs. strain and (b) force vs. strain curves of charge-engineered carbyne chains obtained from DFT calculations with GGA and LDA functional.

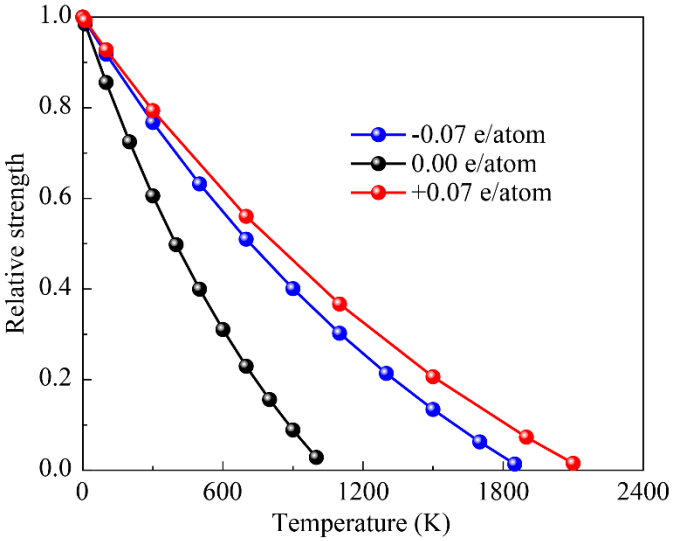

Fig. S6. Relative strength of charged carbyne as a function of temperature.

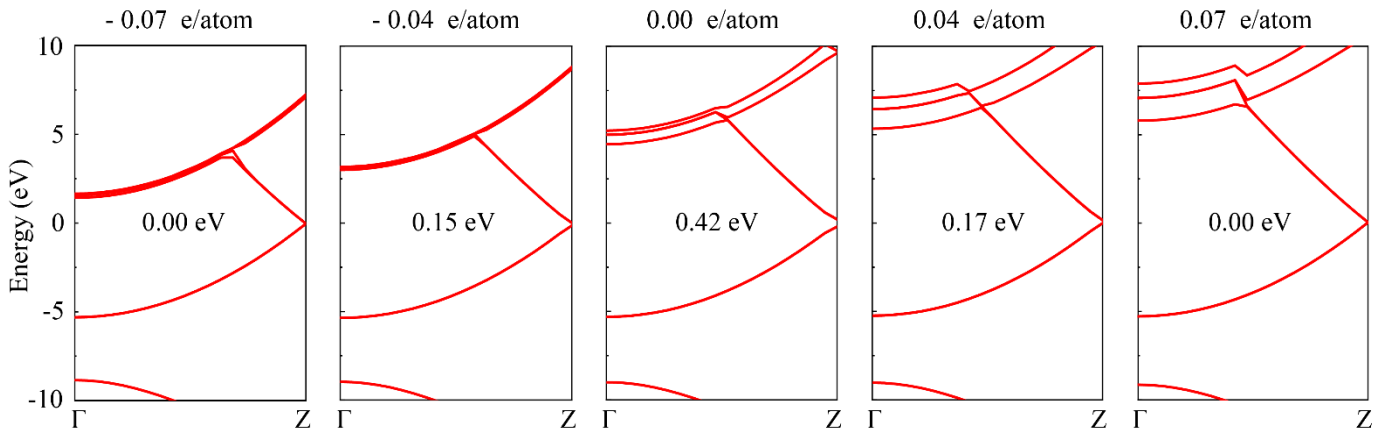

Fig. S7. Band structures of charge-engineered carbyne from DFT calculations.

Table S1. Gravimetric strength (σ_g), gravimetric modulus (Y_g), strain-to-failure (ε_s) and gravimetric toughness of charge-engineered carbyne (CEC) compared with other materials with high mechanical properties.

Crystals	σ_g (GPa·g^{-1}·cm^3)	Y_g (GPa·g^{-1}·cm^3)	ε_s	T (kJ/g)	Refs
CEC (-0.10 e/atom)	101	955	23%	15.4	
CEC (-0.09 e/atom)	102	957	23%	15.5	
CEC (-0.08 e/atom)	102	957	23%	15.6	
CEC (-0.07 e/atom)	103	959	24%	16.7	
CEC (-0.06 e/atom)	78	964	18%	9.9	
CEC (-0.04 e/atom)	77	958	18%	9.7	
CEC (-0.02 e/atom)	75	953	18%	9.5	
CEC (0.00 e/atom)	74	938	18%	9.4	
CEC (+0.02 e/atom)	75	962	18%	9.5	
CEC (+0.04 e/atom)	76	963	18%	9.7	
CEC (+0.06 e/atom)	77	967	18%	9.9	
CEC (+0.07 e/atom)	106	967	26%	19.0	
CEC (+0.08 e/atom)	106	966	26%	19.0	
CEC (+0.09 e/atom)	106	966	26%	19.0	
CEC (+0.10 e/atom)	106	966	26%	19.0	
B chain	76	643	31%	17.0	
BC chain	92	802	25%	15.3	
BN chain	78	868	14%	6.5	
CNT (5, 5)	45	441	30%	10.2	
BNNT (5, 5)	41	349	28%	8.2	
h-BN (zigzag)	45	344	28%	7. 7	[1-3]
Graphene	51	453	25%	8.8	[4]
MoS2 (armchair)	5	40	26%	0.8	[5,6]
Diamond	24	327	13%	2.0	[4]
Lonsdaleite	37	377	31%	8.6	[7,8]
w-BN	26	249	23%	4.1	[9-11]
c-BN	24	230	22%	3.6	[11-13]
BC_3	34	165	23%	4.4	[14]

Movie S1: Ab initio molecular dynamics simulations of charged carbyne at 300 K for 10 ps.

220706MovieS1.mp4

References

[1] Hao T, Zhang Z, Ahmed T, Xu J, Brown S, and Hossain Z M 2021 *J. Appl. Phys.* **129** 014304

[2] Wang R, Pan W, Jiang M, Chen J, and Luo Y 2002 *Mater. Sci. Eng. B* **90** 261

[3] Wu J T, Wang B L, Wei Y J, Yang R G, and Dresselhaus M 2013 *Mater. Res. Lett.* **1** 200

[4] Shao Q, Li R, Yue Z, Wang Y, and Gao E 2021 *Chem. Mater.* **33** 1276

[5] Gan Y Y and Zhao H J 2014 *Phys. Lett. A* **378** 2910

[6] Worsley M A, Shin S J, Merrill M D, Lenhardt J, Nelson A J, Woo L Y, Gash A E, Baumann T F, and Orme C A 2015 *ACS Nano* **9** 4698

[7] Kulnitskiy B, Perezhogin I, Dubitsky G, and Blank V 2013 *Acta. Crystallogr. B. Struct. Sci. Cryst. Eng. Mater.* **69** 474

[8] Li Q, Sun Y, Li Z, and Zhou Y 2011 *Scr. Mater.* **65** 229

[9] Deura M, Kutsukake K, Ohno Y, Yonenaga I, and Taniguchi T 2017 *Jpn. J. Appl. Phys.* **56** 030301

[10] Sōma T, Sawaoka A, and Saito S 1974 *Mater. Res. Bull.* **9** 755

[11] Zhang R F, Veprek S, and Argon A S 2008 *Phys. Rev. B* **77** 172103

[12] Bohr S, Haubner R, and Lux B 1995 *Diamond Relat. Mater.* **4** 714

[13] Richter F, Herrmann M, Molnar F, Chudoba T, Schwarzer N, Keunecke M, Bewilogua K, Zhang X W, Boyen H G, and Ziemann P 2006 *Surf. Coat. Technol.* **201** 3577

[14] Liu X, Zhang G, and Zhang Y W 2015 *J. Phys. Chem. C* **119** 24156